Green Synthesis of Electrochemically Active Silver Nanoparticles

MALATHI, G.,[1] THILLAIYADI VALLIAMMAI, C.,[1]* RIZWANA BEGUM, S.,[2] VINAYAKA, K. S.,[3] VINO UDAPPUSAMY[4] and NIRMALA, P.[5]

[1]Department of Chemistry, A.V.V.M. Sri Pushpam College (Autonomous), Poondi-613503, Thanjavur,
(Affiliated to Bharathidasan University, Tiruchirappalli-24), Tamil Nadu, India.
[2]Department of Biochemistry, Justice Basheer Ahmed Sayeed College for Women (Autonomous)
Chennai, Tamil Nadu, India.
[3]Department of Botany, Sri Venkataramana Swamy College, Dakshina Kannada, Karnataka, India.
[4]Department of Biochemistry, PSG College of Arts & Science, Coimbatore, Tamil Nadu, India.
[5]Department of Microbiology, Hindustan College of Arts & Science, Chennai, Tamil Nadu, India.
*Corresponding author E-mail: thillaiyadivalli@gmail.com

ABSTRACT

The manufacturing of silver nanoparticles (AgNPs) is now safer, more economical, nontoxic, and environmentally benign thanks to the extraction of *Cirsium japonicum*. The extracts from *C. japonicum* worked as a stabiliser and reducer. AgNP synthesis was verified by UV/Vis spectroscopy. There have been studies done on the production of AgNP at various temperatures and concentrations. Their dispersion was validated by high resolution transmission electron microscopy (HRTEM), which also revealed their tiny (2–8nm) spherical form, lack of aggregation, and spherical shape. AgNPs were found to be crystalline using X-ray diffraction (XRD). Using EDX, it was possible to determine the substance's elemental makeup. FTIR spectroscopy was used to identify the chemical molecules that coat AgNPs. The photodegradation of bromo phenyl blue has been investigated in a variety of settings, including experimental setups and catalyst size and structure. In about 12 min, 98 percent of the bromo phenyl blue was destroyed using AgNPs as photo catalysts. Water purification and the transformation of organic hazardous substances into non-hazardous products are obvious uses for AgNPs due to their powerful reductive capabilities. Amazing electro-catalytic abilities for hydroquinone were shown by the electrode (Ag/GC) that was transformed to AgNPs. In an acetate buffer solution, the cyclic voltametric analysis of AgNPs was examined. The experiment findings for GC and modified AgNPs were contrasted. The conductivity of AgNPs was investigated in an acetate buffer solution with a 0.15 M concentration. The generated AgNPs are uniform in size and stability. The produced AgNPs' electrochemical potential was shown.

Keywords: Bromo phenyl blue, Photo degradation, Non-hazardous materials,
Organic hazardous.

INTRODUCTION

Because of their potent antibacterial qualities, silver nanoparticles (AgNPs) are frequently used in consumer goods like clothes, cosmetics, and food storage containers[1]. Many

various kinds of bacteria adversely harm silver, as is widely known. Currently, a number of applications for silver composites with slow silver release rates are being researched[2]. Nanomaterials are increasingly being exploited as a result of their distinct physical and chemical properties[3]. Due to their peculiar optical, electrical, and catalytic capabilities, metallic nanoparticles have been the subject of recent material chemistry study. These biomolecular compounds can be coupled with a variety of useful nanomaterials, such as drugs, ligands, and antibodies with potential biological applications. The physiochemical and biological characteristics of silver-based nano products are distinct from those of other metal nanoparticles. Food, drugs, biomedical imaging, cosmetics, polymers, bactericidal and fungicidal chemicals, and food have all used it. Without a doubt, the ion discharge from the crystalline centres of silver nanoparticles increases their toxicity[6]. Catalytic processes have grown in significance as a result of expanding energy, environmental, and resource challenges[7]. Nanomaterials feature more edges, corners, and high energy than their bulk counterparts, making them more reactive. The usage of silver nanoparticles in commercial products and their discharge into the environment have drawn significant interest from the scientific and regulatory sectors. Both an old and new issue, silicon dioxide discharge into the environment[8]. Green nanoparticle syntheses are presently getting a lot of interest since they are more environmentally friendly than chemical and physical synthesis because they use non-hazardous solvents and reagents. Metal nanoparticles play a key role in nanotechnology because of their unique physical and chemical properties, such as catalytic activity and cutting-edge electrical, magnetic, and optical capabilities[9–12].

Although many conventional techniques were used to create nanoparticles, chemical approaches were most frequently used. The hazardous chemicals used in chemical reduction techniques make nanoparticles unsuitable for biological uses. Nanoparticles' physical, chemical, and biological properties are significantly influenced by their size, shape, morphology, and dispersion. Chemical synthesis is the most common way for creating many nanoparticles quickly and with exact control over particle size distribution[15].
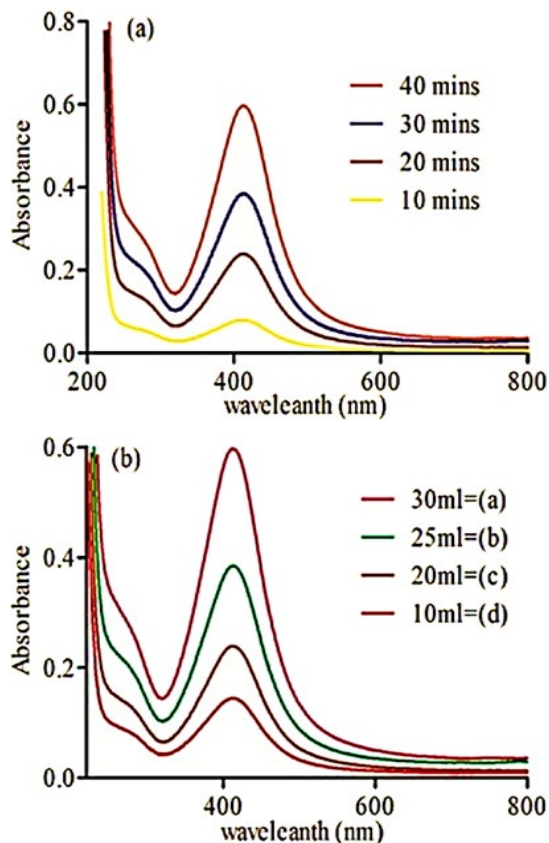

Fig. 1(a). Ag nanoparticles' time-dependent UV-Vis spectra, and (b) the UV-Vis spectra of silver nanoparticles made from various extract concentrations

Biosynthetic nanoparticles can be produced by fungi[16], bacteria[17], plants[18–29], and algae[30]. Numerous industries, including electronics, catalysis, material science, biomedicine, cosmetics, pharmaceuticals, environmental analysis, and remediation, heavily utilize noble metal nanoparticles (NPs)[36]. Their strong reactivity, high surface-to-volume ratio, and tunable optical characteristics are to blame for this. The ability of chemically altered electrodes to detect significant compounds is well recognized[37–40]. Different electrodes have occasionally been employed to electrochemically reduce oxygen. Both the electro catalytic oxygen reduction on plumbagin modified GCEs[44] and the pH-dependent oxygen reduction on multiwall carbon nanotube modified GCE were reported to occur at physiological pH settings. the pH-dependent oxygen reduction on multiwall carbon nanotube modified G., the electro reduction of oxygen to water at "wired" Pleurotus ostreatus laccase cathode[42], and the

electro reduction of oxygen to water at mediated Melano-Carpus Albomyces laccase cathode[41]. Using the aqueous extract of *C. japanicum*, the current experiment generated equally distributed AgNPs. The photocatalytic degradation of bromo phenyl blue was investigated using the recently created AgNPs. In addition, the electrochemical oxidation of hydroquinone by AgNPs derived from green materials was studied. In this study, silver nanoparticles are phytosynthesized using *Cirsium japonicum*, and the electrochemical properties of the electrode modified with silver nanoparticles are characterized.

MATERIALS AND METHODS

Preparation of Cirsium japoni cum extract

To get rid of any dust, *C. japonicum* was repeatedly washed in distilled water at *Musa khel* in Bannu, Pakistan. Using demonic water at a rate of 250 revolutions per minute for 39 min, 50 g of the dust-free plant material were extracted. After 10 min of centrifugation at 5000rpm with filter paper, the supernatant was collected and utilised. As a reducing and stabilizing agent, AgNPs were produced from the resulting clear filtrate.

Synthesis of silver nanoparticles

A 200 mL beaker containing 50 mL of a 3 103 M aqueous solution of silver nitrate and 10 mL of C was used to create AgNPs. Japaneseium aq extract. By switching from white to black in less than 80 min, AgNPs were investigated. The resulting black color is a definite indicator that AgNPs are starting to develop. The black color is visible due to the surface Plasmon resonance of the AgNPs. It was possible to watch the growth of nanoparticles using UV-Vis spectroscopy. The AgNPs suspension was repeatedly separated from the water for 20 min at 10,000rpm using centrifugation.

Photo catalytic activity

Tests for photocatalytic activity were conducted using bromophenyl blue decomposition in aqueous solution. The light source was a UV-light. AgNPs were dissolved in 60 mL of bromo phenyl blue solution (15 mg/L) with the addition of 9 mg of AgNPs.
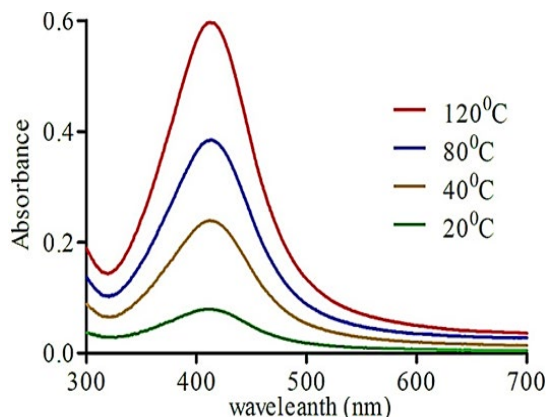

Fig. 2. EffectoftemperatureduringAgNPsformation

In addition, an AgNP-free control configuration was discovered. After 35 min of dark magnetic stirring, the working solution was in equilibrium before being exposed to radiation. As soon as the suspension was created, the bromo phenyl blue solution was placed under UV light, and the rate of deterioration was then checked every 30 min after that. At 614nm, a Shimadzu 2450 UV-V spectrophotometer was used to track the decline of BPB. The equation was used to determine the degradation percentage.
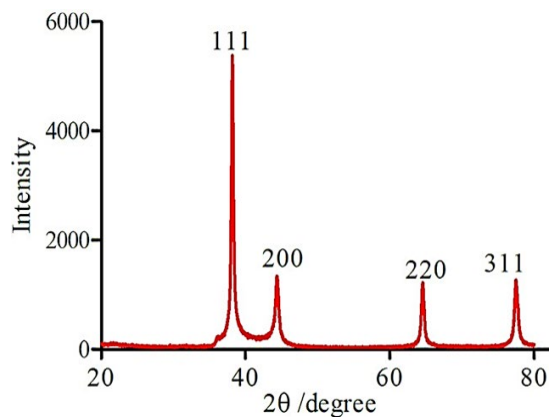
Degradation % = $\frac{1}{4}^{\delta Ac-AtP} \times 100$

Fig. 3. XRDpatternsofthesynthesizedAgNPs

While blank (control) has an absorbance of Ac, test has an absorbance of At. Using a blank test, the dye's self-degradation under visible light was also assessed.

Characterization studies

The biogenesis of silver nanoparticles was monitored using a UV-2450 spectrophotometer

(Shimadzu) with a resolution of 1nm in the wavelength range of 350-800nm. The Rigaku Miniflex X-ray diffractometer was used to evaluate the XRD pattern between 10 and 70 degrees. The appearance, size, and crystal structure of Ag nanoparticles were investigated using a JEOL3010 high resolution transmission electron microscope and a Hitachi EDX elemental microanalysis equipment. The infrared (IR) spectrum of Ag nanoparticles was acquired using a transmittance mode with a resolution of four centimeters on an ABB MB3000 spectrophotometer.

Cyclic voltametric evaluation of an electrode modified with AgNPs

The glassy carbon electrode (GCE) was ultrasonically washed in methanol to create a mirror-like finish after being polished with alpha Al_2O_3 to a 5mm diameter. The AgNPs and activated charcoal that had been dissolved in the polished GC electrode at room temperature were free of the solvent. The resultant GC/AgNPs were subsequently described. Using a disinfectant, loosely bound AgNPs were removed from the modified GC electrode. The experiment that follows made use of this modified electrode.

Voltammetry in cycles

For the cyclic voltametric analysis, the electrochemical workstations CS-300 and CHI-600 were utilized. In this measurement, 5mm-diameter glassy carbon electrodes (GCEs) and modified GCEs were used as working electrodes, Pt wires were used as a counter electrode, and saturated calomel electrodes (SCEs) were used as standards. Glassy carbon electrodes modified with AgNPs have electrocatalytic activity.

The redesigned electrode was evaluated electrochemically in an electrolyte medium with a 0.15 M sodium acetate solution (CV). In order to assess the electrocatalytic performance of biogenic AgNPs, cyclic voltammetry was performed (CV). The CV responses of the phenol catechol $C_6H_6O_2$ in 0.15 M sodium acetate solution were compared using a glassy carbon electrode (GCE) at room temperature and an AgNPs-assembled glassy carbon electrode (SCE) at room temperature. The electrochemical breakdown of BPB was studied in an aqueous sodium acetate solution using modified AgNPs as the working electrode.
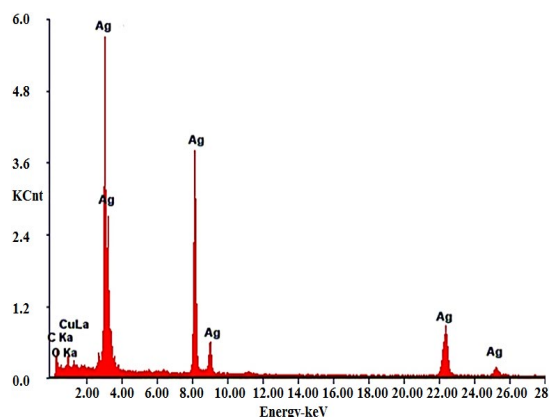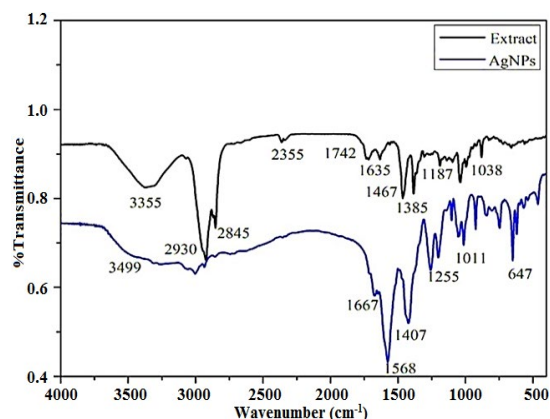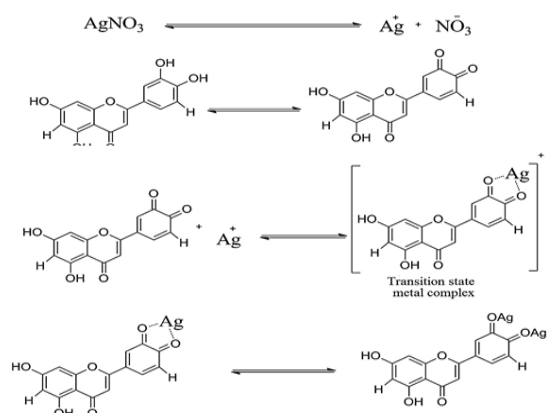

Fig. 4. EDXanalysesofAgNPs

Fig. 5. FT-IR spectrum recorded by making KBr pellet with synthesized AgNPs nanoparticles


Scheme 1. Typical proposed mechanisms of silver nanoparticles formation of *C. japonicum* extracts

### RESULTS & DISCUSSION

UV–Vis spectroscopy

UV/Visible spectroscopy was used to track the rate of Ag nanoparticle synthesis. Metal nanoparticle SPR patterns can be discovered using

UV-Visible spectroscopy. The phenomenon known as SPR occurs when the conduction band electrons of metal nanoparticles collectively vibrate in resonance at a particular wavelength of the illuminating light. Fig. 1a demonstrates how the UV/Visible spectral monitoring was time-dependent. As shown in Fig. 1a, the SPR peak becomes more intense and sharper as contact time increases. SPR indicates that the absorbance peaked at 447nm. AgNPs' environment, size, and shape dispersion all have an impact on their SPR peak. For metallic nanoparticles between 2 and 100nm in size, SPR produces a peak that has been thoroughly investigated[45]. The effects of several plant extracts on the synthesis of AgNPs are shown in Fig. 1b. An SPR band at 430nm was discovered as soon as 10 mL of plant extract was added to the silver precursor. At this quantity of plant extract, a very low absorbance was observed, which showed that few nanoparticles had formed. However, when 20 mL of the plant extract were employed, the SPR peaks' intensities rose.
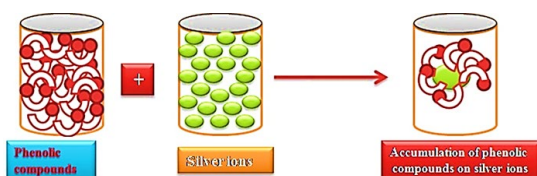
Scheme 2. Diagrammatic depiction of silver nanoparticle formation

The particle size might grow even larger if the plant concentration was raised further. An increase in the polyphenolic content may account for the larger particle size observed at higher plant concentrations. According to earlier research, these molecules are necessary for the production of nanoparticles[46]. Everything here indicates an increase in the production of silver nanoparticles with a restricted size distribution.
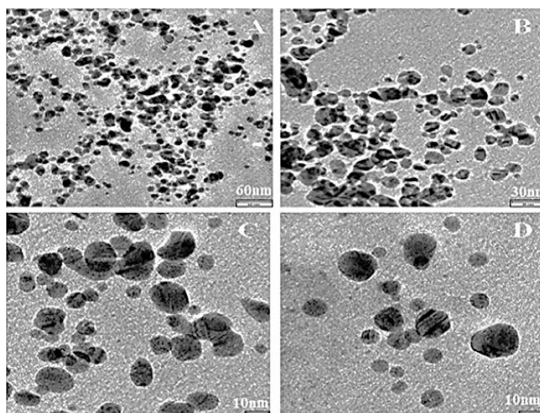
Fig. 6. HRTEM images of *C. japonicum* extracts prepared with AgNPs at various concentrations (A) 30 mL, (B) 25 mL, (C) 20 mL, and (D) 10 mL

Effect of temperature on their action rate

The AgNPs were heated to different temperatures before having their surface plasmon resonance spectra collected, as seen in Fig. 2. The peak's sharpness increased from 20 to 40°C, suggesting that there may have been an increase in reaction time. The produced nanoparticles' small size is what causes the peak to be so sharp[48]. If the extract's reducing and stabilising power is diminished when heated above 80°C, it may only have a limited capacity to stabilise at higher temperatures. It is conceivable that organic Compounds break down at temperatures below 100°C since the majority of organic substances are stable there. the diagram of X-ray diffraction.

X-ray diffraction (XRD) pattern

As shown in Fig. 3, XRD analysis was used to determine the crystal structure of the synthesized AgNPs. The Bragg reflection peaks of 38.21°, 44.30°, 64.52°, and 77.47° of face-centered cubic silver, respectively, indicate the 111, 200, 220, and 311 lattice planes. The observation at 2=38.21 is in agreement with the cubic AgNPs with faces[49], shows a significant peak. The findings of this study show that the 111 plane is the top crystal plane (basal plane) in the creation of nanoparticles. Due to its high atomic density, the 111 facet is regarded to be the most reactive. Silver and gold nanoparticles have previously been shown to exhibit a similar diffraction pattern when reduced and covered with plant extract[50]. The following Debye-Eq. Scherrer's law illustrates how the FWHM (full width half maximum) of the diffraction peaks was also used to determine the typical crystal size of these particles. The Scherrer's constant in this instance is d14K=cos K. is the ray's X-wavelength. The symbols for the Braggs' angle and the half-breadth of the peak are and, respectively.

X-ray with energy dispersion (EDX)

The EDX profile, which displayed substantial signals in the 3 keV range and is a characteristic signal for the absorption of metallic and spherical nano crystals due to surface plasmon resonance[51,52], corroborated the elemental composition of silver nano crystals. A high silver nanoparticle yield was achieved because there was no longer any ionic silver (Ag⁺) signal, indicating that all of the Ag⁺ had been transformed to Ag°. FT-IR analysis and EDX patterns demonstrate that *C. japonicum* extract is

used to decrease silver ions and produce crystalline AgNPs. The functional groups responsible for the reduction and capture processes have been located in the aqueous extract of *C. japonicum* using FT-IR analysis. Aqueous extracts of *C. japonicum* and silver nanoparticles produced by *C. japonicum* are shown in Fig. 5. The infrared spectra at the following wavelengths, in that order: 3355 cm^{-1}, 2930 cm^{-1}, 2930 cm^{-1}, 2355 cm^{-1}, and 3355 cm^{-1}, reveal one of the most notable properties of the *C. japonicum* aqueous extract. The -OH stretching-related vibrational peaks are located at 3355 cm^{-1}. As far as we can tell, amide II's NH stretching vibration, as well as the C-O stretch and C-N stretch, are contained in the extra peaks at 2930, 1385, and 1083 cm^{-1}. An apparent decrease in peak intensities in the FT-IR spectra of AgNPs produced by *C. Japanicum* suggests that these groups may be involved in the synthesis and stability of AgNPs. The flavonoids' -C O stretching vibration decreased from 1640 to 1670 cm^{-1}, the AgNPs' O-H stretching vibration increased from 3355 to 3499 cm^{-1}, and amid II's NH stretching vibration increased from 2922 to 2921 cm^{-1} [54–55].
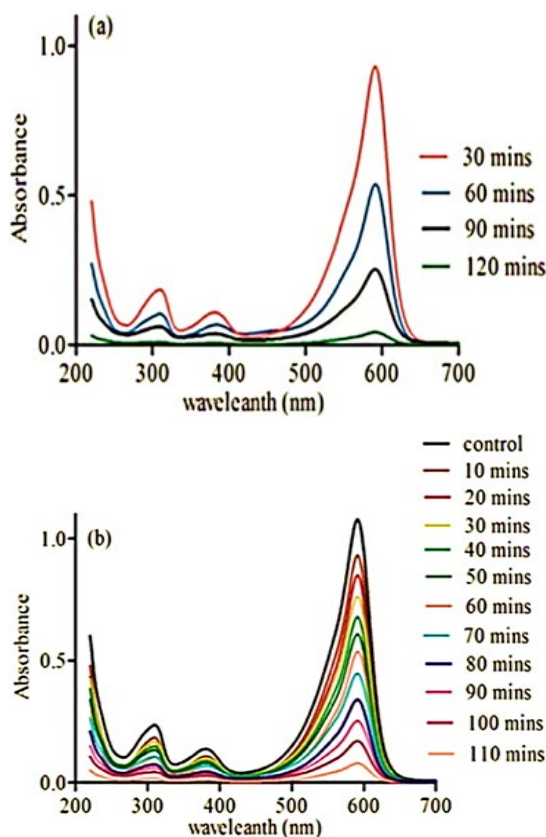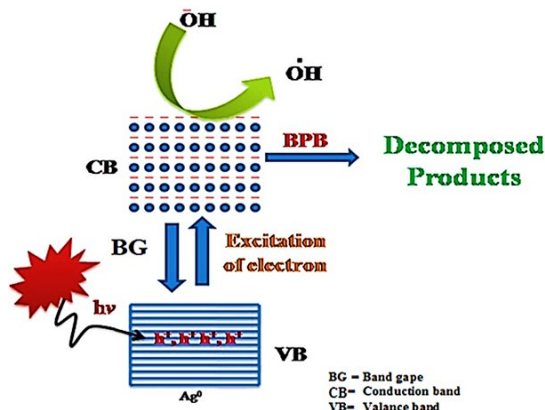

Fig. 7. AgNPs' photocatalytic activity as it relates to the photodegradation of bromophenylblue is time-dependent

Scheme 3. Mechanism of photo degradation of bromophenylblue (BPB)byAgNPs

These findings suggest that a number of functional groups, including proteins, flavonoids, and saponins, present in the phenolic components of the Japani cum aqueous extract, may stabilize the AgNPs generated. These alcoholic chemicals' hydroxyl groups may support silver's bio-reduction. The FT-IR spectrum of Fig. 5 shows that -OH groups, which are present in Cirsium species[56], are essential for the synthesis and stabilization of AgNPs. It has been proposed[51,52] to employ *C. japonicum* extract as a reducing and stabilizing agent for the manufacture of AgNPs. Schemes 1 show the proposed process for making AgNPs.

High resolution transmission electro n microscopy

Using HRTEM, the produced AgNPs' size, shape, morphology, and dispersion were all studied. The morphology of the silver nanoparticles matches the form of the SPR band in the UV-Vis spectrum, which is perfectly visible in the HRTEM image. The estimated particle size from the XRD analysis and the average particle size from the HRTEM images, which ranges from 4 to 8nm, are well matched. Fig. 6 shows the spherical and highly dispersed AgNPs, and the HRTEM findings, which are consistent with the EDX results, show no signs of aggregate formation. Because of their large surface area, increased number of active sites, smaller, spherical particle size, and good dispersion, AgNPs exhibit excellent electrocatalytic and photocatalytic activities[57,58].

Photo degradation of bromophenylblue (BPB)

For the sake of the environment, AgNPs' photocatalytic efficiency must be increased.

Numerous industries pollute the environment with dye and other organic substances, putting people, plants, and animals in peril. The breakdown of BPB, one of the colouring agents, necessitates a number of circumstances because it is a stable organic chemical with a big aromatic molecular structure that is particularly resistant to heat and light. Since BPB has such a negative impact on the environment, scientists

must do critical research on this topic and address a significant problem. Nanoparticles are extremely valuable for degrading these waste products. In this experiment, the photo catalytic activity of AgNPs was assessed using the model compound bromo phenyl blue. The degradation of photographs was assessed using bromo phenyl blue, which demonstrated a distinct absorption peak at 630 nanometers.
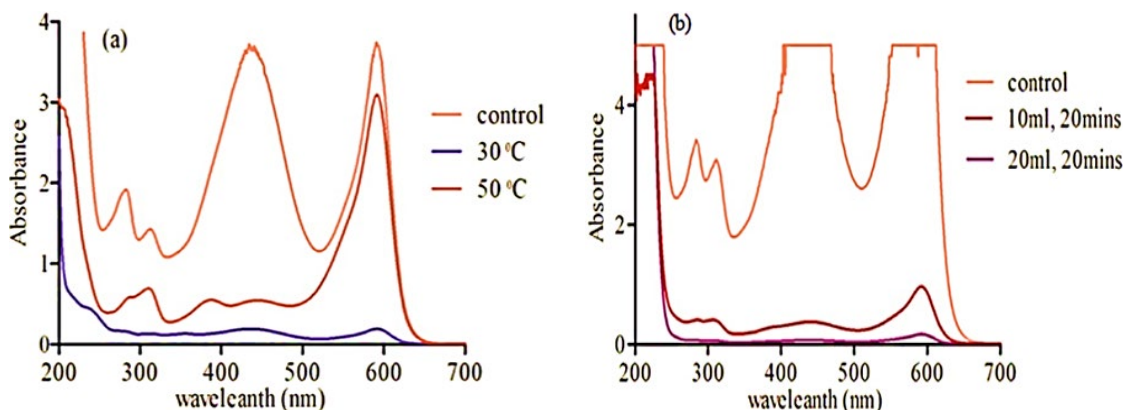

Fig. 8(a). Effect of concentration of AgNPs on the degradation of bromophenyl blue (b) Effect of temperature on the degradation of bromophenyl blue
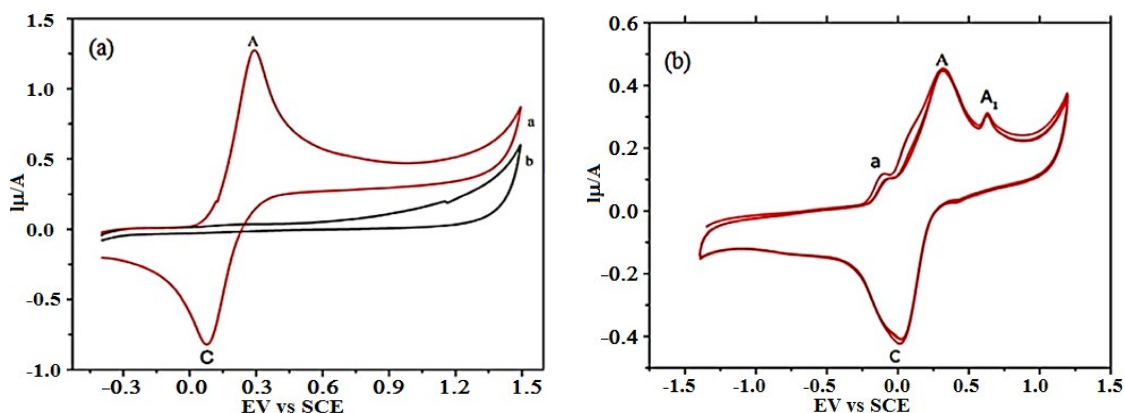

Fig. 9(a). Cyclic voltammograms of catechol on GCelectrodein 0.15M sodium acetate solution.Ats canning rate 50m V-s⁻¹ vs SCE at 25°C. (b) Multicyclic voltammetry of catechol atGC/AgNPs modified past electrode scanning rate 50m V-s⁻¹ vs SCEat25°C

The examination of the absorption spectra of BPB aqueous solutions over time in the presence of AgNPs is depicted in Fig. 7a and 7b. In the presence of AgNPs and light, it was observed that the main absorption peak shrank, indicating photodegradation of BPB. AgNPs have a stronger photodegradation property for three reasons. The first justification is that AgNPs do a superior job of light absorption. Due to their small size, silver particles have more active sites and can cover a bigger surface area. The third cause is high dispersion

without any agglomeration. Particle morphology, crystal structure, and size all significantly affect photo catalytic activity, according to studies[59,60]. The mechanism that has been postulated up to this point is shown in Scheme 3 and involves AgNPs breaking down BPB photocatalytically. The idea was that when the AgNPs were exposed to UV light, the valence electrons in their valence shell would be freed. These more powerful electrons produce hydroxyl radicals, hastening the breakdown of BPB. AgNPs concentrations and temperature effects.

The photodegradation of bromo phenyl blue was examined by increasing the concentration of AgNPs in the solution from 5 to 10 mg, as shown in Fig. 8a. The outcomes are displayed in UV radiation was used in this experiment for 20 min at room temperature (see inset in Fig. 8a). The breakdown of bromo phenyl blue increased from 80% to 98% when the amount of AgNPs was increased from 5 to 10 mg. From 15 to 20 mg of AgNPs, the efficiency of AgNPs' photodegradation decreased, showing that AgNPs' capacity for photodegradation decreased with concentration. Smaller, scattered particles provide more surface area and active sites for AgNPs' photodegradation against BPB at lower concentrations than larger, dispersed particles. Between 5 mg and 10 mg, the photodegradation activity of the AgNPs significantly decreased. The agglomeration of AgNPs at higher concentrations, which increased particle size, resulted in a decrease in the specific surface area of the particles and the number of surface-active sites. The highest photodegradation efficiency for bromo phenyl blue was found to be 10 mg of AgNPs. As seen in Fig. 8b, temperature has an effect on BPB photodegradation. The degradation of BPB is directly influenced by

temperature. At 30°C, only 15% of BPB was degraded; at 50°C, breakdown reached 98%. The degradation of BPB by the AgNPs was discovered to be more significant than their paralyzing effect, as seen in Figure 8b.

Electro chemical behavior of catecholatAg-NPs modified electrode

Utilizing cyclic voltammetry, the electrocatalytic activity of biosynthesised AgNPs was evaluated. Fig. 9a shows the catechol $C_6H_6O_2$ CV responses at the glassy carbon electrode (GCE), in contrast to the saturated calomel electrode (SCE). Anodic and cathodic peaks in Fig. 9a have similar intensities.[61–66] This states that the electrolytically produced highly reactive species qunonine (2a) is oxidized to catechol. This highly reactive species' stability on an electrode surface was also shown by the redox pair[64–66]. Catechol-modified AgNPs were studied using multi-cycle cyclic voltammetry in a 0.15 M sodium acetate electrolyte. The anodic peaks at 0.1, 0.45, and 0.53 V slightly lost power during the circular scanning[65-68]. "a," which occurred at a lower voltage, demonstrated the stability of the o-qunonine produced during the electrochemical oxidation of catechol.
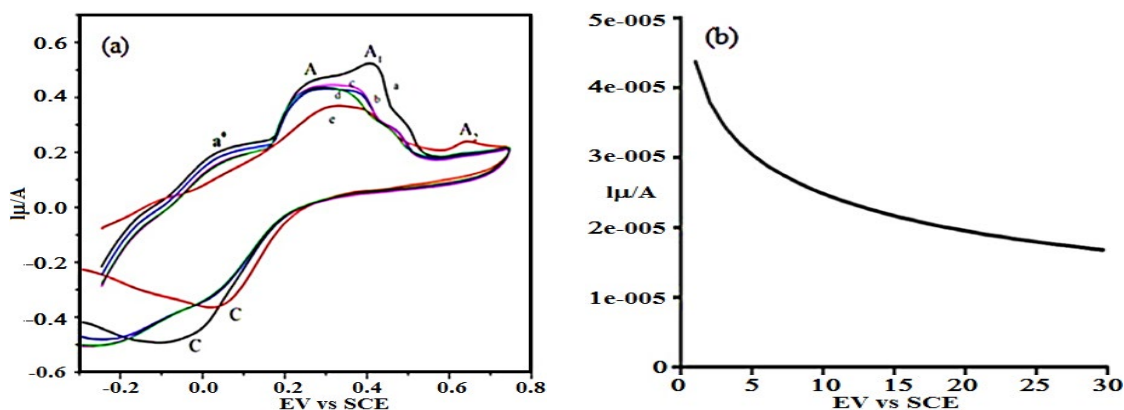

Fig. 10. Effect of scanning at 100, 80, 60, 50, and 20 mV/s⁻¹ on the breakdown of BPB at GC/AgNPs modified electrode at 25°C vs. SCE in cyclic voltammetric studies of BPB in 0.15 Macetate aqueous solution (a)

Effect of linear weep potential of modified paste vs SCE at 25°C

Because of the equilibrium between 1a and 2a, as shown in Fig. 9b, the peak appeared to be declining with lower scanning. Two anodic peaks (A and A1) are observed during the electrochemical oxidation of phenolic compounds, proving that the process is a 2e, reversible one[67,68]. Scheme 3[66] shows both the

anodic conversion of catechol to o-qunonine and the reverse conversion of qunonine to catechol. There was no difference in peak intensity between the second and third cycle because, as Scheme 4 illustrates, the equilibrium between 1a and 2a had been reached. The electrochemical oxidation of catechol to o-quinine provided the best sensitivity for the GC-modified electrode, as can be seen in Figure 9b.

Deprivation of bromophenylblue by electro chemical method using glassy carbon-AgNPs modified electrode

Cyclic voltametric analysis in aqueous media with a 0.15 M acetate buffer solution was used to evaluate the degradation of BPB[53] using the modified GC/AgNPs electrode shown in Fig. 10. When heated to 25°C and scanned at speeds between 100 and 80 mV/s^{-1}, BPB liquefied more quickly than SCE (as depicted in Fig. 10a). The BPB showed two anodic peaks and one cathodic peak at different potentials when scanning more quickly (A, A1 and C). During electrochemical reactions in aqueous conditions, an additional "a°" peak appeared at 0.3 V, proving the stability of the produced intermediate. The electrochemical reaction resulted in three C peaks at 2.5, 4.2, and 0.7 V, two anodic and one cathodic. Anodic peaks (A and A1) are produced by the cathodic peak (C), which represents the opposite process, and require a higher voltage than those produced by the intermediate oxidation shown in curve. This is brought on by the intermediate's stability in an aquatic setting. The redox process in IpA/IpC is analogous to that in electrochemical processes[61-68]. Slower scanning rates reduce the anodic and cathodic peaks because BPB concentration is reduced as BPB is electrochemically broken down. It is shown that the potential of Peak A2 is higher while scanning at a rate of 20 mV/s^{-1}. At a scanning rate of 20 mV/s^{-1}, the BPBs seem to be completely degraded to their corresponding products. A2 may be produced by electrochemical techniques such as polymerization or hydroxylation[65]. Scheme 5 displays the anticipated electrochemical breakdown of BPB.
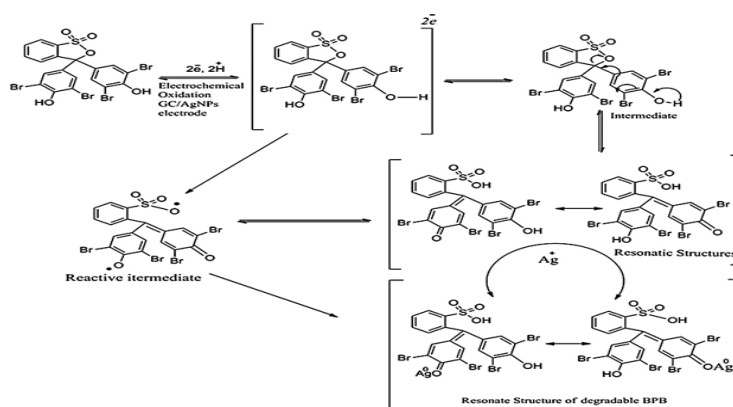
Scheme 5. Bromo phenyl blue's electrochemical dilapidation by 0.15 M acetate aqueous. The mechanism is proposed to be buffer solution on a modified GC-AgNPs electrode at 25°C

CONCLUSION

Using *C. japonicum* extract as a reductor and stabilizer, a bio-green technique that is cost-effective and ecologically friendly was used to create the well dispersed, stable, and electrochemically active AgNPs. The plant extract can be used to make nanoparticles with particular sizes and morphologies. By using XRD and EDX, the AgNPs' FCC structure and elemental composition were confirmed. The HRTEM results showed that the AgNPs were tiny, spherical, and broadly distributed at low plant extract concentrations. Ag-NP produced through biosynthesis has different diameters depending on the reaction duration. As a result, Ag-NP size increases at room temperature as reaction time increases. Silver nanoparticles have been found to be highly effective and sensitive electrocatalysts. In other words, the redox process and other phenolic applications benefit from the electrocatalytic capabilities of Ag/GC. This process may generate AgNPs without the use of any dangerous chemicals, making it appropriate for electrochemical and medicinal applications. The BPB was successfully removed from water by the synthetic AgNPs. To better understand how BPB and other colours (organic pollutants) are electrochemically broken down by AgNPs during water filtration, more research is urgently required.

REFERENCES

1. Zong-Ming Xiu.; Jie Ma.; Pedro J. J. Alvarez, Differential effect of common ligands and molecular oxygen on antimicrobial activity of silver nanoparticles versus silverions, *Environ. Sci. Technol.*, **2011**, *45*, 9003–9008.

2. Thiel. J.; Pakstis. L.; Buzby. S.; Raffi. M.; Ni. C.; Pochan. D. J.; S. Ismat Shah Titania.; *Antibacterial properties of silver-doped titania, Small.,* **2007***, 3*(5), 799–803.

3. Albrecht. M. A.; Evans. C. W.; Raston. C. L.; *Green chemistry and the health implications of nanoparticles, Green Chem.,* **2006**, *8*, 417–432.

4. Mody. V. V.; Siwale. R.; Singh. A.; Mody. R. H.; Introduction to metallic nanoparticles, *J. Pharm. Bioallied Sci.*, **2010**, *2*, 282–289.

5. Prabhu. S.; Poulose. E. K.; Silver nanoparticles: mechanism of antimicrobial action, synthesis, medical applications, and toxicity effects, *Int. Nano Lett.*, **2011**, *2*, 1–10.

6. Bindhu. M. R.; Umadevi. M.; Antibacterial and catalytic activities of green synthesizedsilver nanoparticles, *Spectrochim. Acta A Mol. Biomol. Spectrosc.*, **2015**, *135*, 373–378.

7. Ma. Rui; Clement Levard.; Gordon, E. Brown Jr.; Stella, Marinakos. M.; Gregory, Lowry. V.; Size controlled dissolution of silver nano particles, *Environ.Sci.Technol.*, **2012,** *46*, 752–759.

8. Zong-ming Xiu.; Qing-bo Zhang.; Hema L. Puppala.; Vicki L. Colvin.; Pedro J. Alvarez.; Negligible particle-specific antibacterial activity of silver nanoparticles, *Nano Lett.*, **2015**, *12*(8), 4271–4275.

9. Voloktitin. Y.; Sinzig.J. ; Jong. L. J.; Schmid. G.; Vargaftik. M. N.; Moiseev. I. I.; Quantum-sizeeffects in the namic properties of metallic nanoparticles, *Nature.*, **1996**, *384*, 621–623.

10. Shipway. A. N.; Katz. E.; Willner. I.; Nanoparticle arrays on surfaces for electronic, optical, and sensor applications, *Chem Phys Chem.*, **2000,** *1*, 18–52.

11. Hayward. R. C.; Saville. D. A.; Aksay. I. A.; Electrophoretic assembly of colloidal crystals with optically tunable micro patterns, *Nature.,* **2000**, *404*, 56–59.

12. Lala. N. L.; Ramaseshan. R. ; Bojun. L.; Sundarrajan. S.; Barhate. R.; Ying-jun. L.; Fabrication of nanofibers with antimicrobial functionality used as filters: protection against bacterial contaminants, *Biotechnol. Bioeng.*, **2007,** *97*, 1357–1365.

13. Sundarrajan. S.; Chandrasekaran. A. R.; Ramakrishna. S.; An update on nanomaterials-based textiles for protection and decontamination, *J. Am. Ceram. Soc.*, **2010,** *93*, 3955–3975.

14. Gade Aniket.; Swapnil Gaikwad.; Nelson Duran.; Mahendra Rai.; Green synthesis of silver nanoparticles by phomaglomerata, *Micron, 2014*, *59*, 52–59.

15. Kowshik. M.; Ashtaputre. S.; Kharrazi. S.; Vogel. W.; Urban. J.; Kulkarni. S. K.; Paknikar. K. M.; Extra cellular synthesis of silver nanoparticles by a silver-tolerant yeast strain MKY3,*Nanotechnology.,* **2003***, 14*, 95–100.

16. Mukherjee. P.; Ahmad. A.; Mandal. D.; Senapati. S.; Sainkar. S. R.; Khan. M. I.; Parishcha. R.; Ajaykumar. P. V.; Alam. M.; Kumar. R.; Sastry M., Fungus-mediated synthesis of silver nanoparticles and their immobilization in the mycelial matrix: a novel biological approach to nanoparticle synthesis, *Nano Lett.*, **2001**, *1*, 515–529.

17. Mandal. D.; Bolander. M. E.; Mukhopadhyay. D.; Sarkar. G.; Mukherjee. P., The use of mi-croorganisms for the formation of metal nanoparticles and their application, *Microb. Biotechnol.*, **2006**, *69*, 485–492.

18. Arif Ullah Khan.; Yun Wei.; Zia Ul Haq Khan.; Kamran Tahir.; Shahab Ullah Khan.; Aftab Ahmad.; Faheem Ullah Khan.; Li Cheng.; Qipeng Yuan.; *Int. J. Electrochem. Sci.,* **2015**, *10*, 7905–7916.

19. Kamran Tahir.; Sadia Nazir.; Baoshan Li.; Arif Ullah Khan.; Zia Ul Haq Khan.; Aftab Ahmad.; Qudrat Ullah Khan., **2015**, *09*, 015.

20. Kamran Tahir.; Sadia Nazir.; Baoshan Li.; Arif Ullah Khan.; Zia Ul Haq Khan.; Yu Gong Peng.; Shahab Ullah Khan.; Aftab Ahmad.; *Mater. Lett.*, **2015**, *156*, 198–201.

21. Aftab Ahmad.; Fatima Syed.; Akram Shah.; Zahid Khan.; Kamran Tahir.; Arif Ullah Khan.; Qipeng Yuan.; *RSC Adv.*, **2015**, *5*, 73793–73806.

22. Kamran Tahir.; Sadia Nazir.; Baoshan Li.; Arif Ullah Khan.; Zia Ul Haq Khan.; Aftab Ahmad.; Faheem Ullah Khan.; *S ep. Purif.Technol.*, **2015**, *150*, 316–324.

23. Zia Ul Haq Khan.; Amjad Khan.; Afzal Shah.; Yongmei Chen.; Pingyu Wan.; Arif UllahKhan.; Kamran Tahir.; Nawshad Muhammad.; Faheem Ullah Khan.; Hidayat Ullah Shah.; *J. Photochem. Photobiol. B Biol.*, **2016**, *156*, 100–107.

24. Kamran Tahir.; Baoshan Li.; Shafiullah Khan.; Sadia Nazir.; Zia Ul Haq Khan.; Arif UllahKhan.; Rafiq UlIslam.; *J. Alloys Compd.,* **2015**, *651*, 322–327.

25. Arif Ullah Khan.; Qipeng Yuan.; Yun Wei.; Shahab Ullah Khan.; Kamran Tahir.; Zia UlHaq Khan.; Aftab Ahmad.; Farman Ali Khan.; Shafqat Ali.; Sadia Nazir.; *RSC Adv.*, **2016**, *6*, 23775.

26. Arif Ullah Khan.; Yun Wei.; Aftab Ahmad.; Zia Ul Haq Khan.; Kamran Tahir.; Shahab Ullah Khan.; Nawshad Muhammad, Faheem Ullah Khan.; Qipeng Yuan.; *J. Mol. Liq.*, **2016**, *215*, 39–46.

27. Arif Ullah Khan.; Yun Wei.; Zia Ul Haq Khan.; Kamran Tahir.; Aftab Ahmad.; Shahab Ullah Khan.; Faheem Ullah Khanl.; Qudrat Ullah Khan.; Qipeng Yuan. *Separation Science and Technology.*, **2016**, *114*, 0203.

28. Arif Ullah Khan.; Qipeng Yuan.; Yun Wei.; Zia ul Haq Khan.; Kamran Tahir.; Shahab Ullah Khan.; Aftab Ahmad.; Shafi ullah Khan.; Sadia Nazir.; Faheem Ullah Khan.; *J. Photochem. Photobiol.BBiol.,* **2016***, 159*, 49–58.

29. Ahmad. N.; Sharma. S.; Alam. M. K.; Singh. V. N.; Shamsi. S. F.; Mehta. B. R.; A Rapid syn-thesis of silver nanoparticles using dried medicinal plant of basil, *Colloids Surf*. B., **2010,** *81*, 81–86.

30. Bankar. B.; Joshi. A. R.; Kumar. A. R.; Zinjarde. S.; Banana peel extract mediated novelroute for the synthesis of silver nanoparticles, Colloids Surf. *A Physicochem. Eng. Asp.*, **2010**, *368*, 58–63.

31. Bar. H.; Bhui. D. K.; Sahoo. G. P.; Sarkar. P.; De. S. P.; Pyne. S.; A Green synthesis of silver nanoparticles using seed extract of Jatrophacurcas, *Misra Colloids Surf.A*3., **2009**, *48*, 212–216.

32. Iravani. S.; Green synthesis of metal nanoparticles using plants, *Green Chem.*, **2011**, *13*, 2638–2650.

33. Palanivel Velmurugana.; Subpiramaniyam Sivakumar b.; Song Young-Chaec.; Jang Seong-Hob.; YiP young-Inb.; SuhJeong-Minb.; Hong Sung-Chulb.; Synthesis and characterization comparison of peanut shell extract silver nanoparticles with commercial silver nanoparticles and their antifungal activity, *J. Ind. Eng. Chem.*, **2015**, *31*, 51–54.

34. Mubarak Ali. D.; Thajuddina. N.; Jeganathan. K. ; Gunasekaran. M.; Plant extract mediated synthesis of silver and gold nanoparticles and its antibacterial activity against clinically isolated pathogens, *Colloids Surf.B.,* **2011***, 85*, 360–365.

35. Chelladurai Karuppiah.; Selvakumar Palanisamy.; Shen-Ming Chen.; R. Emmanuel.; M.Ajmal Ali.; P. Muthukrishnan, P. Prakash.; FahadM. A. Al-Hemaid, Greenbiosynthesisof silver nanoparticles and nanomolar detection of p-nitrophenol, *J. Solid State Electrochem.*, **2014**, *18*, 1847–1854.

36. Mohsin Nawaz.; Dongwoo Kim.; Waheed Miran.; Avinash Kadam.; Jun Heo.; Seolhye Shin.; Jiseon Jang.; Seong-Rin Lim.; Dae Sung Lee.; Effect of toluene.; an immiscible pol-lutant, on the photocatalytic degradation of azo dye, *J. Ind. Eng. Chem.*, **2015**, *30*, 10–13.

37. Murray. R. W.; Ewing. A. G.; Durst. R. A.; Chemically modified electrodes. Molecular de-sign forelectro analysis, *Anal.Chem.*, **1987**, *59*, 379A–390A.

38. Shakkthivel. P.; Chen. S.-M.; Simultaneous determination of ascorbic acid and dopamine in the presence of uric acid on ruthenium oxide modified electrode, *Biosens. Bioelectron.*, **2007**, *22*, 1680–1687.

39. Thiagarajan. S.; Tsai. T.-H.; Chen. S.-M.; Easy modification of glassy carbon electrode for simultaneous determination of ascorbicacid, dopamineanduric acid, *Biosens. Bioelectron.*, **2009**, *24*, 2712–2715.

40. Kavanagh. P.; Jenkins. P.; Leech.D. ; Electro reduction of O_2 at mediated melanocarpusalbo myceslaccasecathodeina physiological buffer, *Electrochem. Commun.*, **2008**, *10*, 970–972.

41. Barton. S. C.; Pickard. M.; Duhal. R. V.; Heller. A.; Electroreduction of O_2 to water at 0.6 V(SHE) at pH7 on the "wired" Pleurotus ostreatus laccase cathode, *Biosens. Bioelectron.*, **2002**, *17*, 1071–1074.

42. Kruusenberg.; Alexeyeva. N.; Tammeveski. K.; The pH-dependence of oxygen reduction on multi-walled carbon nano tube modified glassy carbon electrodes, *Carbon.,* **2009**, *47*, 651–658.

43. Ardakani. M.M.; Karami. P. E.; Zare. H. R.; Hamzehloo. M.; Electrocatalytic reduction of oxygen on the surface of glassy carbon electrodes modified with plumbagin, *Microchim. Acta.,* **2007**, *159,* 165–173.

44. Gutierrez. M.; Henglein. A.; Formation of colloidal silver by "push–pull" reduction ofsilver(1+), *J. Phys. Chem.*, **1993**, *97*, 11368–11370.

45. Kumar. V.; Yadav. S. C.; Yadav. S. K.; *Syzygium cmini* leaf and seed extracts of Partheniumhysterophorus:a novel biological approach, *J. Chem.Technol. Biotechnol.*, **2010**, *85*, 1301–1309.

46. Philip. D.; Biosynthesis of Au, Ag and Au–Ag nanoparticles using edible mushroomextrct, *Spectrochim. Acta.*, **2009**, *A73*, 374–381.

47. Fayaz. A. M.; Balaji. K.; Kalaichelvan. P. T.; Venkatesan. R.; Fungal based synthesis of sil-ver nanoparticles-an effect of temperature on the size of particles, *Colloids Surf.*, **2009**, *B74*, 123–126.

48. P. D. D. Files, JCPDS International Center for Difraction Data, Pennsylvania, PA., **1991**.

49. Nasrollahzadeh. M.; Sajadi. S. M.; Babaei. F.; Maham. M.; *Euphorbia helioscopia* Linn as a green source for synthesis of silver nanoparticles and their optical and catalyticproperties, *J. Colloid Interface Sci.*, **2015**, *450*, 374–380.

50. Magudapathy. P.; Gangopadhyay. P.; Panigrahi. B.; Nair. K.; Dhara. S.; Electrical trans-port studies of Ag nano clusters embedded in glass matrix, *Phys. B Condens. Matter.,* **2001,** *299*, 142–146.

51. Muthukrishnan. S.; Bhakya. S.; Kumar. T. S.; Rao. M.; Biosynthesis, characterization and anti-bacterial effect of plant-mediated silver nanoparticles using Ceropegiathwaitesii-an endemic species,*Ind.Crop. Prod.*, **2015**, *63*, 119–124.

52. Stuart. B. H.; Infra-red spectroscopy: fundamentals and applications., **2004**, 71–93.

53. Tokonami. S.; Morita. N.; Takasaki. K.; Toshima. N.; Novel synthesis, structure, and ox-idation catalysis of Ag/Au bimetallic nanoparticles, *J. Phys. Chem. C.,* **2010**, *114*,

10336–10341.

54. J. Li.; Xu. J.; Dai. W. L.; Li. H.; Fan. K.; Directhydro-alcohol thermal synthesis of special core–shell structured Fe-doped titania microspheres with extended visible light re-sponse and enhanced photo activity, *Appl. Catal. B Environ.*, **2009**, *85*, 162–170.

55. Zia Ul Haq Khan.; Yongmei Chen Shafiullah Khan.; Pingyu Wan.; *In vitro* antimicrobial activity of the chemical constituents of *Cirsiumarvense*(L).Scope,*J.Med.Plant Res.*, **2013**, *7*(25),1894–1898.

56. Chandran. S. P.; Chaudhary. M.; Pasricha. R.; Ahmad. A.; Sastry. M.; Synthesis of goldnanotriangles and silver nanoparticles using Aloe vera plant extract, *Biotechnol. Prog.*, **2006**, *22*, 577–583.

57. Sathyavathi. R.; Krishna. M. B.; Rao. S. V.; Saritha. R.; Rao. D. N.; Biosynthesis of silver nanoparticles using *Coriandrum sativum* leaf extract and their application in non-linearoptics, *Adv. Sci. Lett.*, **2010**, *3*, 1–6.

58. Huang. J.; Li. Q.; Sun. D.; Lu. Y.; Su. Y.; Yang. X.; Wang. H.; Wang. Y.; Shao. W.; He. N.; Bio-synthesis of silver and gold nano particles by novel sundried *Cinnamomum camphora* leaf, *J NanoTechnol.*, **2007**, *18*, 105104–105115.

59. Roy. N.; Mondal. S.; Laskar. R. A.; Basu. S.; Mandal. D.; N. A. Begum, Biogenic synthesis of Au and Ag nanoparticles by Indian propolis and its constituents, *Colloids Surf. B:Biointerfaces.,* **2010**, *76*, 317–325.

60. Mogyorósi. K.; Balázs. N.; Srankó. D.; . Tombácz. E; Dékány. I.; Oszkó. A.; Sipos. P.; Dombi. A.; The effect of particle shape on the activity of nanocrystalline TiO_2 photocatalysts in phenol decomposition. Part 3: the importance of surface quality, *Appl. Catal.B Environ.*, **2010**, *96*, 577–585.

61. Saha. S.; Pal. A.; Kundu. S.; Basu. S.; Pal. T.; Photochemical green synthesisofcalcium-al-ginate-stabilized Ag and Au nanoparticles and thei rcatalytic application to 4-nitro-phenol reduction, *Langmuir.,* **2009**, *26*, 2885–2893.

62. Nematollahi. D.; Golabi. S. M.; Electro chemical study of catechol and 4-methyl catecholin methanol. Application to the

electro-organic synthesis of 4,5- dimethoxy-
and 4-methoxy-5-methyl-o-benzoquinone,
J. Electroanal. Chem., **1996**, *405*,133–140.

63. Zia Ul Haq Khan.; Yongmei Chen.; Shafiullah
Khan.; Dandan Kong.; Mo Heng Liang.;
Pingyu Wan.; Electrochemical initiation
of nucleophilic substitution of hydroqui-
nonewith4,6-dimethyl pyrimidine-2-thiol, *Int.
J. Electrochem. Sci.*, **2014**, *9*, 4665–4674.

64. Davood. S.; Mahdi Golabi.; Nematollahi.;
Investigation of the electromethoxyl at
ion reaction part 2: electrochemical study
of 3-methyl catechol and 2,3-dihydr oxy
benzaldehyde in methanol, *Electroanalysis.*,
2001, *12*, 1008–1015.

65. Zia Ul Haq Khan.; Arif Ullah Khan.; Yongmei
Chen.; Shafiullah Khan.; Dandan Kong.;
Karman Tahir.; Faheem Ullah Khan.; Pingyu
Wan.; Jin Xin.; Electrochemical oxidation of
catechols in the presence of 4-mercapto-
benzoic acid, to synthesis sulfanyl com-
pounds and their biological studies,
Tetrahedron., **2015**, *71*, 1674–1678.

66. Silverstein. R.; Webster. F. X.; Spectrometric
identification of organic compounds, John
Wiley & Sons, New York., **1998,** 217–249
(Chapter 6,6thend).

67. Nematollahi. D.; Golabib. S. M.; Investigation
of the electro-methoxyl at ion reaction part 1.
Electrochemical study of 4-tert-butyl catechol
and 3,4-dihydroxy benzal dehydein methanol,
J.Electroanal.Chem., **2000**, *481*, 208–214.